JOURNAL OF VIROLOGY, Oct. 2006, p. 9424–9434 Vol. 80, No. 19
0022-538X/06/$08.00+0 doi:10.1128/JVI.00768-06

Resistance to Alpha/Beta Interferon Is a Determinant of West Nile Virus Replication Fitness and Virulence

Brian C. Keller,[1] Brenda L. Fredericksen,[1] Melanie A. Samuel,[2] Richard E. Mock,[3] Peter W. Mason,[4] Michael S. Diamond,[2] and Michael Gale, Jr.[1]*

Department of Microbiology, University of Texas Southwestern Medical Center, Dallas, Texas 75390-9048[1]; Departments of Medicine and Molecular Microbiology, Washington University School of Medicine, St. Louis, Missouri 63110[2]; Texas Veterinary Medical Diagnostic Laboratory, Amarillo, Texas 79116-3200[3]; and Department of Pathology, University of Texas Medical Branch, Galveston, Texas 77555-0436[4]

Received 14 April 2006/Accepted 18 July 2006

The emergence of West Nile virus (WNV) in the Western Hemisphere is marked by the spread of pathogenic lineage I strains, which differ from typically avirulent lineage II strains. To begin to understand the virus-host interactions that may influence the phenotypic properties of divergent lineage I and II viruses, we compared the genetic, pathogenic, and alpha/beta interferon (IFN-α/β)-regulatory properties of a lineage II isolate from Madagascar (MAD78) with those of a new lineage I isolate from Texas (TX02). Full genome sequence analysis revealed that MAD78 clustered, albeit distantly, with other lineage II strains, while TX02 clustered with emergent North American isolates, more specifically with other Texas strains. Compared to TX02, MAD78 replicated at low levels in cultured human cells, was highly sensitive to the antiviral actions of IFN in vitro, and demonstrated a completely avirulent phenotype in wild-type mice. In contrast to TX02 and other pathogenic forms of WNV, MAD78 was defective in its ability to disrupt IFN-induced JAK-STAT signaling, including the activation of Tyk2 and downstream phosphorylation and nuclear translocation of STAT1 and STAT2. However, replication of MAD78 was rescued in cells with a nonfunctional IFN-α/β receptor (IFNAR). Consistent with this finding, the virulence of MAD78 was unmasked upon infection of mice lacking IFNAR. Thus, control of the innate host response and IFN actions is a key feature of WNV pathogenesis and replication fitness.

West Nile virus (WNV) is a positive-sense single-stranded RNA virus in the family *Flaviviridae*. Isolates of WNV are subdivided into two lineages: lineage I viruses are represented by emergent strains distributed throughout the world and have been associated with outbreaks of encephalitis and meningitis in Europe, the Middle East, and, most recently, in North America, whereas lineage II isolates are largely nonemergent/endemic strains that are confined to the African subcontinent and the island countries of Madagascar and Cyprus (5, 7, 25, 26). In most cases, WNV infection of humans can be characterized as asymptomatic or as a mild, febrile illness termed West Nile fever. However, a significant increase in the global incidence of severe neurological disease associated with WNV lineage I infections arose in the mid-1990s, culminating in the U.S. outbreak in 2003, which included 9,862 reported cases and 264 deaths (CDC website, http://www.cdc.gov/ncidod/dvbid/westnile/index.htm). After its introduction in New York City in 1999, WNV rapidly spread across the continent and now appears to have firmly established itself in the ecology of North America. The rapid emergence of WNV and its virulence within a naïve population suggest that epidemic forms of the virus may encode mechanisms to evade host immunity.

Infection with WNV triggers a delayed host response that includes the activation of interferon regulatory factor-3 (IRF-3) and the subsequent production of alpha/beta interferon (IFN-α/β) (14, 15, 38). IFNs are a family of immunomodulatory cytokines that are produced in response to virus infection and serve as integral signal initiators of host intracellular defenses (40, 46). Binding of IFN to the cognate IFN-α/β receptor (IFNAR) on target cells results in the activation of the JAK-STAT pathway, which includes the receptor-associated kinases JAK1 and Tyk2 that in turn phosphorylate and activate their downstream effectors, STAT1 and STAT2. Activated phospho-STAT1/STAT2 heterodimers translocate to the nucleus to form a heterotrimeric complex with IRF-9 and induce the transcription of hundreds of interferon-stimulated genes (ISGs), whose products can direct antiviral and antiproliferative actions that limit virus replication and spread. Many viruses encode proteins that direct mechanisms to disrupt innate antiviral defenses and IFN-induced JAK-STAT signaling, and these processes have been linked to viral emergence in new host populations and species (16, 23, 44) and to pathogenic outcomes of infection (reviewed in references 11, 40, and 46). Importantly, virulent isolates of WNV have been shown to be capable of attenuating IFN actions by preventing STAT1 and STAT2 activation, although the mechanisms of this regulation and its influence in vivo were not defined (17, 29). Here we describe in vitro and in vivo studies comparing the genetic and phenotypic properties of a lineage I/emergent strain and a lineage II/nonemergent strain of WNV. Our data show that viral control of IFN action and JAK-STAT signaling is critical for high replication fitness and virulence. We propose that WNV control of IFN defenses may provide a platform for pathogenesis and continual emergence within naïve host populations.

* Corresponding author. Mailing address: University of Texas Southwestern Medical Center, 5323 Harry Hines Blvd., Dallas, TX 75390-9048. Phone: (214) 648-5940. Fax: (214) 648-5905. E-mail: Michael.Gale@UTSouthwestern.edu.

MATERIALS AND METHODS

Cells, viruses, and IFN. Vero, A549, Huh7, HEK-293, and wild-type and IFN-α/β receptor-deficient mouse embryo fibroblast (MEF) cell lines were propagated in Dulbecco's modified Eagle medium (DMEM) supplemented with 10% fetal bovine serum (FBS), 2 mM L-glutamine, 1 mM sodium pyruvate, antibiotic-antimycotic solution, and 1× nonessential amino acids (complete DMEM). Preparation of WNV strain NY 2000-crow3356 (NY 3356) (GenBank accession number AF404756) working stocks from plasmid pFLWNV was previously described (15). WNV isolate TX 2002-HC (TX02) was isolated on Vero cells inoculated with brain homogenate from an infected grackle (*Quiscalus quiscula*) that was recovered from Hall County in the Texas Panhandle. Virus was amplified once in HEK-293 cells, and supernatants were collected and stored frozen for further analyses of viral stocks. WNV strain Madagascar-AnMg798 (MAD78) was obtained from the World Reference Center of Emerging Viruses and Arboviruses (5) and passaged once in Vero cells. Working stocks of TX02 and MAD78 were obtained by plaque purifying virus and amplifying one time in HEK-293 cells at a low multiplicity of infection (MOI). For IFN treatment, A549 cells were incubated in the presence (pretreatment) or absence (posttreatment) of increasing doses of IFN-α-2a (PBL Biomedical Laboratories) for 24 h prior to infection with TX02 or MAD78. Following 1 h of virus adsorption, inoculum was replaced with medium containing IFN-α-2a. At indicated times postinfection, culture supernatants and whole-cell lysates were collected for analysis by plaque assay on Vero cells and immunoblotting, respectively. For analysis of JAK-STAT signaling components, A549 cells were infected with TX02 or MAD78 (MOI = 5) for 1 h, and inoculum was replaced with complete DMEM. At indicated times, complete DMEM was replaced with complete DMEM containing IFN-α-2a (1,000 U/ml) for 0, 15, or 30 min, and whole-cell lysates were collected for immunoblot analysis.

Sequencing and phylogenetic analysis of WNV strains. Monolayers of Vero cells were infected (MOI = 0.5) with TX02 or MAD78 for 1 h at 37°C with rocking. At 24 (TX02) or 48 (MAD78) h postinfection, total RNA was collected using TRIzol LS (Invitrogen) according to the manufacturer's instructions. cDNA synthesis was performed on 2 μg RNA using random nonamers (IDT) and Omniscript reverse transcriptase (QIAGEN) for 90 min at 37°C. Overlapping PCR products were obtained initially using primers designed from the sequence of NY 3356 (for TX02) or a lineage II consensus sequence created from the alignment of the Uganda 1937, B956, and Sarafend sequences (for MAD78). Secondary internal sequence-specific primers were used to amplify PCR fragments spanning the initial primer regions to eliminate any bias from the NY 3356- or lineage II consensus-specific primers. Sequencing was performed with PCR products by use of Applied Biosystems Inc. (ABI) BigDye Terminator 3.1 chemistry and ABI capillary instruments. This protocol was repeated for both viruses to confirm sequence data. Alignment of the amino acid sequences encoded by the entire WNV open reading frame was done using CLUSTAL W (43). Distances were estimated with the amino acid transition probability matrix of Jones, Taylor, and Thornton (21). Neighbor-joining phylogenetic trees were constructed using MOLPHY, version 2.3, with maximum likelihood rearrangement (1). Bootstrap values in support of branches are the result of 1,000 neighbor-joining replicates. Japanese encephalitis virus isolate HW (JE HW) (GenBank accession number AY849939) was used as the out-group.

Plaque assays and virus growth analysis. Monolayers of Vero, A549, or Huh7 cells were washed twice in serum-free media. Cells were infected with 10-fold serial dilutions of virus for 1 h at 37°C with rocking. Inoculum was removed and replaced with a 0.9% agarose overlay. Forty-eight h later, a second 0.9% agarose overlay containing 2% Neutral Red (ICN Biomedicals) was added to the cells. Plaques were counted at 48 (TX02) or 96 (MAD78) h after the second overlay. All plaque assays were performed in duplicate. For analysis of virus growth kinetics, A549 or Huh7 cells were infected with NY 3356, TX02, or MAD78 at MOIs of 1 based on titers determined on the respective cell line. At the indicated times, culture supernatants were recovered from infected cultures, and the level of infectious virus was determined by plaque assay on Vero cells. In parallel, cells were harvested and whole-cell lysates were prepared for immunoblot analysis. All growth curve determinations were performed multiple times, and viral titration analyses were conducted in duplicate for each sample.

Protein analyses. Proteins (30 to 35 μg) were analyzed by immunoblotting as previously described (15). The following primary antibodies were used to probe the blots: mouse anti-WNV from the Centers for Disease Control; rabbit anti-ISG56, kindly provided by Ganes Sen; rabbit anti-phosphotyrosine 1054/1055 Tyk2, rabbit anti-phosphotyrosine 1022/1023 JAK1, rabbit anti-phosphotyrosine 701 STAT1, rabbit anti-STAT1, and rabbit anti-PARP from Cell Signaling; rabbit anti-Tyk2 and rabbit anti-phosphotyrosine 689 STAT2 from Upstate; and mouse anti-STAT1α, rabbit anti-STAT2, goat anti-actin, and goat anti-GAPDH from Santa Cruz. Secondary antibodies included peroxidase-conjugated goat anti-rabbit, goat anti-mouse, and donkey anti-goat (Jackson Immunoresearch). Immunoprecipitation of JAK1 was performed by infecting A549 cells (MOI = 5) as described above. Twenty-four h postinfection, cells were pulsed with 1,000 U IFN-α-2a for 0, 15, or 30 min and then collected in buffer A (25 mM Tris-Cl [pH 7.5], 150 mM NaCl, 1% NP-40) plus 1 μM okadaic acid, 1 μM phosphatase inhibitor cocktail II (Calbiochem), and 10 μM protease inhibitor (Sigma). Lysates were immunoprecipitated with mouse anti-phosphotyrosine (Cell Signaling) or mouse anti-JAK1 (BD Biosciences) antibodies and protein A agarose beads (Roche) and analyzed by immunoblotting with the opposite antibody. For cell extract fractionation experiments, A549 cells were mock infected or infected with WNV. Twenty-four h later, the cells were pulse treated with 1,000 U IFN-α-2a for 1 h in complete DMEM. Cytoplasmic and nuclear fractions were collected and analyzed by sodium dodecyl sulfate-polyacrylamide gel electrophoresis and immunoblotting. Cytoplasmic lysis buffer consisted of 10 mM Tris-HCl, 60 mM KCl, 1 mM EDTA, 2 mM dithiothreitol, and 0.15% NP-40. Nuclear extract buffer consisted of 20 mM Tris-Cl, 400 mM NaCl, 1.5 mM $MgCl_2$, 0.2 mM EDTA, and glycerol. For the indirect immunofluorescence assay of protein localization, A549 cells were seeded on four-chamber microscope slides (Nalge Nunc International) and infected (MOI = 2) with TX02 or MAD78. Inoculum was replaced with complete DMEM, and incubation was done for 24 h, at the end of which time cells were pulsed with complete DMEM or with complete DMEM containing IFN-α-2a (1,000 U/ml) for 60 min at 37°C. Cells were washed once in phosphate-buffered saline and fixed in 4% paraformaldehyde for 30 min at room temperature. Cells were permeabilized and stained as previously described (15) with fluorescein isothiocyanate-conjugated human anti-WNV (1:400) (kindly provided by Jorge Munoz-Jordan) and rabbit anti-STAT2 (1:100) primary antibodies. Cells were then incubated with goat anti-rabbit rhodamine-conjugated secondary antibody (1:1,000) (Jackson Immunoresearch) and DAPI (4′,6′-diamidino-2-phenylindole) (1:100) and visualized at the UT Southwestern Pathogen Imaging Facility with a Zeiss Pascal LSM confocal microscope with Axiovision software.

Mouse lethality experiments. Commercially obtained 4-week-old outbred Swiss-Webster mice were divided into 10 groups of 10 animals and inoculated intraperitoneally with 100 μl of virus diluted in phosphate-buffered saline containing 10% FBS. The inocula consisted of a Vero passage 1 preparation of NY 385-99 (GenBank accession number AY842931) (kindly provided by Robert Tesh) and a Vero passage 2 preparation of plaque-purified TX02, in both cases diluted to give titers of 1,000, 200, 40, 8, or 1.6 PFU per 100 μl. Following inoculation, animals were monitored for lethality. Moribund animals (defined as those not expected to survive for an additional 24 h) were humanely euthanized and scored as dead the following day. Fifty percent lethal dose values were determined using the method of Reed and Muench (37). Wild-type C57BL/6J mice were obtained commercially. IFNAR-deficient mice ($IFNAR^{-/-}$) on a pure C57BL/6J background were obtained from Jonathan Sprent (Scripps Institute, San Diego, CA) and genotyped. For infection of wild-type C57BL/6J and $IFNAR^{-/-}$ mice, TX02 and MAD78 were plaque purified and passaged twice on Vero cells to generate viral stocks that were used in all experiments. Eight- to 10-week-old wild-type and $IFNAR^{-/-}$ mice were infected by footpad inoculation with 10^2 PFU of each virus diluted in Hanks balanced salt solution with 1% heat-inactivated FBS as described previously (38). Mice were monitored daily for lethality. Mouse experiments were approved and performed in accordance with the guidelines of the UTMB Institutional Animal Care and Use Committee or the Washington University Animal Studies Committee.

Nucleotide sequence accession numbers. The entire coding sequences of WNV TX 2002-AC and WNV Madagascar-AnMg798 have been deposited into the GenBank database with accession numbers DQ176637 and DQ176636, respectively.

RESULTS

Genetic and phenotypic characterization of WNV isolates from Madagascar and Texas. WNV MAD78 was isolated from an infected parrot (*Coracopsis vasa*) in the Analabe region of Madagascar in May 1978 (34). On the basis of a small region of the E gene, Berthet and colleagues proposed that MAD78 clusters with WNV lineage II (7). Expanding on their findings, we determined the complete coding sequence of MAD78 and compared it to those of other WNV strains. In agreement with previous studies (5, 7, 10, 25), phylogenetic analysis of the

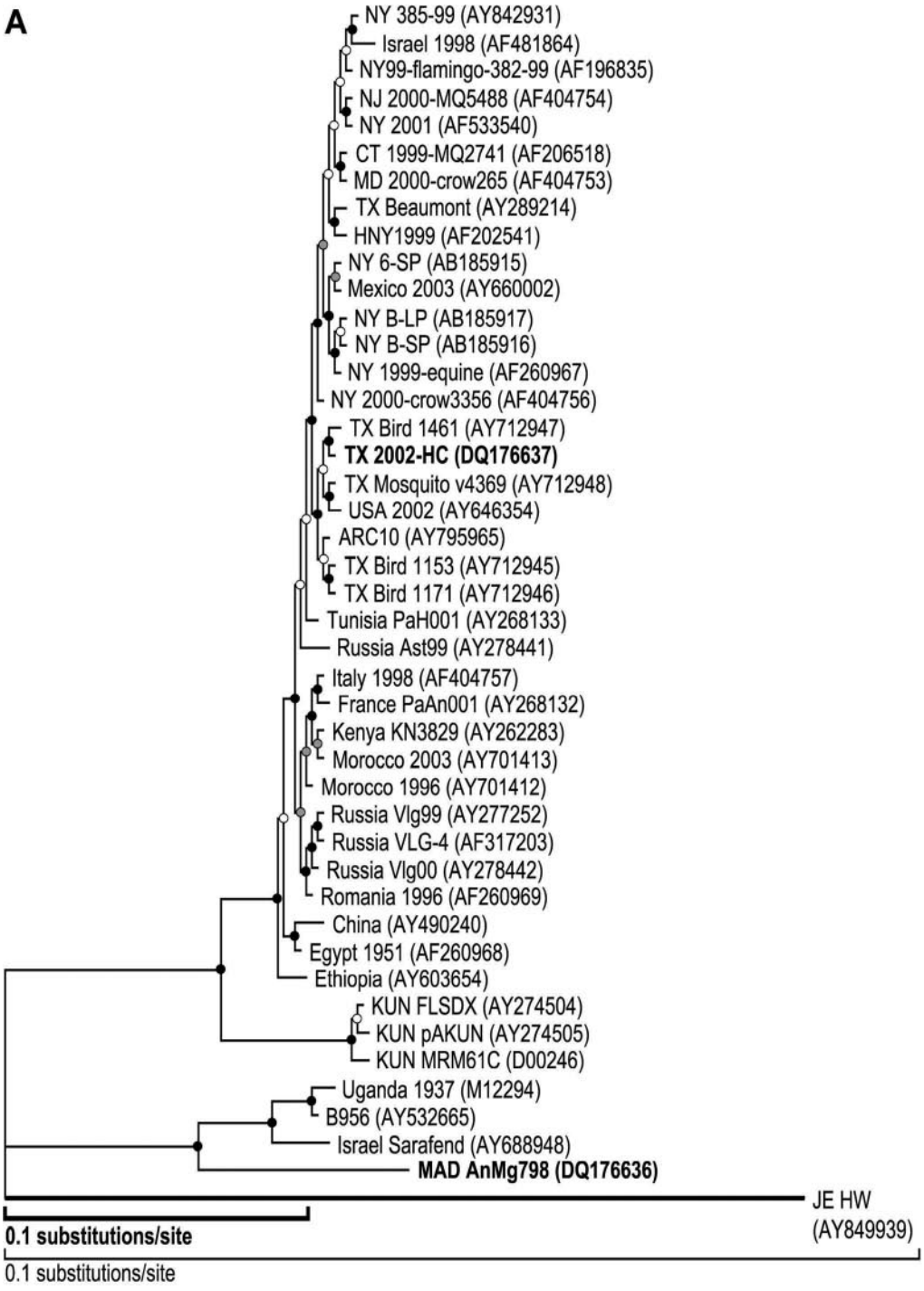

B **Amino acid differences between TX02 and NY99 (upper) or MAD78 and Uganda 1937 (lower)**

Gene	Total	Core	prM/M[a]	E	NS1	NS2a	NS2b	NS3	NS4a	NS4b	NS5
TX02 & NY99											
# aa differences	4	0	1	1	0	0	1	0	0	0	1
% aa identity	99.9	100	99.4	99.8	100	100	99.2	100	100	100	99.9
MAD78 & Uganda 1937											
# aa differences	128	2	3	20	20	22	2	11	4	18	26
% identity	96.3	98.4	98.2	96.0	94.3	90.5	98.5	98.2	97.3	93.0	97.1

[a]prM, premembrane; M, membrane; E, envelope; NS, nonstructural

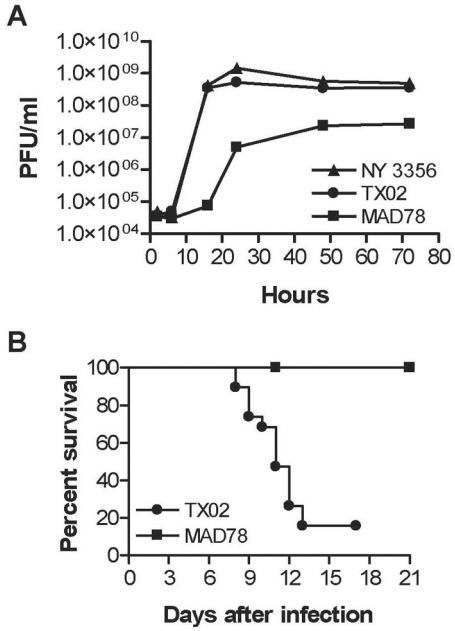

FIG. 2. In vitro and in vivo characterization of MAD78 and TX02. (A) A549 cells were infected (MOI = 1) with TX02, MAD78, or NY 3356. At 2, 6, 18, 24, 48, and 69 h postinfection (TX02, NY 3356) or 2, 6, 16, 24, 48, and 72 h postinfection (MAD78), culture supernatants were collected and the titers of the viruses were determined by plaque assay on Vero cells. (B) Groups of wild-type C57BL/6 mice were infected by footpad inoculation with 10^2 PFU of MAD78 or TX02 and monitored for survival. Results are plotted as percent surviving mice.

entire open reading frame clearly places MAD78 in lineage II (Fig. 1A), although MAD78 appears to cluster genetically distant from other lineage II strains. Across the complete open reading frame, MAD78 exhibits 83.9% (nucleotide) and 96.3% (amino acid) similarity to the lineage II prototype strain from Uganda (Fig. 1B and data not shown).

TX02 was isolated in August 2002 from the brain of an infected grackle (*Quiscalus quiscula*) in Hall County, Texas. Following plaque purification, the entire TX02 coding sequence was determined by use of overlapping reverse transcriptase PCR. Sequence comparison with published complete WNV genomes demonstrated very little genetic divergence between TX02 and other lineage I WNV strains in North America (Fig. 1A). Relative to the prototype 1999 U.S. isolate, WNV NY99-flamingo382-99 (NY99), only four amino acid substitutions (one each in the prM/M, E, NS2b, and NS5 genes) were identified in TX02 (Fig. 1B).

One-step growth analyses of virus replication in human lung carcinoma (A549 [Fig. 2A]) or human hepatoma (Huh7 [data not shown]) cells revealed that TX02 displays growth kinetics and peak infectious virus production nearly identical to those of WNV NY 3356, a well-characterized lineage I strain that is 99.9% identical (25) to the NY99 isolate. By comparison, growth of MAD78 was delayed and peak infectious virus production was decreased 10-fold relative to the lineage I strains. To define the virulence phenotype of TX02, cohorts of outbred Swiss-Webster mice were inoculated by the intraperitoneal route with increasing doses of TX02 or NY 385-99 and monitored for survival (data not shown). We found that both TX02 and NY 385-99, a second control isolate from the 1999 New York outbreak (42), conferred lethality in mice challenged with a dose of 10^3 PFU, resulting in mortalities of 90% (mean survival time of 7.7 days) and 100% (mean survival time of 7.5 days), respectively. Furthermore, we calculated 50% lethal dose values for TX02 and NY 385-99 of 7.1 and 5.8 PFU, respectively, thus confirming the lethality of TX02 in a mouse model. On the other hand, MAD78 demonstrated a nonneuroinvasive, nonpathogenic phenotype in outbred Swiss-Webster mice when inoculated intraperitoneally with doses 10-fold higher than those used in our TX02 experiments (4, 5), consistent with its reduced replication fitness in vitro. Further, in vivo characterization of MAD78 and TX02 by footpad inoculation of inbred C57BL/6 mice with 10^2 PFU resulted in 0% lethality and 86% lethality, respectively ($n = 19$; $P < 0.0001$) (Fig. 2B), confirming the attenuated nature of MAD78.

MAD78 and TX02 exhibit differential responses to interferon action. We hypothesized that the different virulence phenotypes of MAD78 and TX02 may be due, in part, to variable interactions with IFN antiviral defense programs of the host cell. We therefore evaluated the influence of IFN on viral growth. One hour after infection with TX02 or MAD78, cultures of A549 cells were treated with 10 U of IFN-α-2a or with medium alone. We then examined infectious particle production and cell-associated viral protein abundance at various times postinfection and posttreatment. As shown in Fig. 3A, low-dose IFN treatment resulted in 8-fold ($P < 0.03$; paired *t* test) and 1.5-fold ($P = 0.1$; paired *t* test) reductions in peak infectious virus production of MAD78 and TX02, respectively. With low-dose IFN treatment, viral protein abundance was almost completely suppressed in MAD78-infected cells, but levels of TX02 proteins were only slightly affected, if at all, in the presence of IFN (Fig. 3B). Similar patterns of protein expression were observed with higher IFN doses (data not shown). These results demonstrate that MAD78 is highly sensitive to antiviral processes induced by relevant doses of IFN-α-2a, while TX02 is strongly resistant to IFN-induced antiviral actions.

To further analyze the differential responses of MAD78 and TX02 to the antiviral effects of IFN, A549 cells were left untreated or were treated with increasing doses of IFN-α-2a

FIG. 1. Phylogenetic analysis of complete WNV coding sequences. (A) Complete WNV genomic sequences were obtained from GenBank and aligned using CLUSTAL W. The neighbor-joining tree was created by maximum likelihood using MOLPHY, version 2.3, with sequence JE HW as the out-group. Bootstrap values are the result of 1,000 replicates and are represented by shaded dots at the nodes (black, values of ≥90; gray, values of ≥75 but <90; white, values of <75). Scale bars are proportional to genetic distance. Because of the extreme divergence between the JE HW out-group and the WNV isolates, two different scale bars are used. The thick line represents the scale for the JE out-group, while the thin line depicts the relative scale for the WNV isolates. (B) Amino acid comparisons of TX02 to the original WNV NY99 isolate and MAD78 to the prototypical Uganda 1937 isolate.

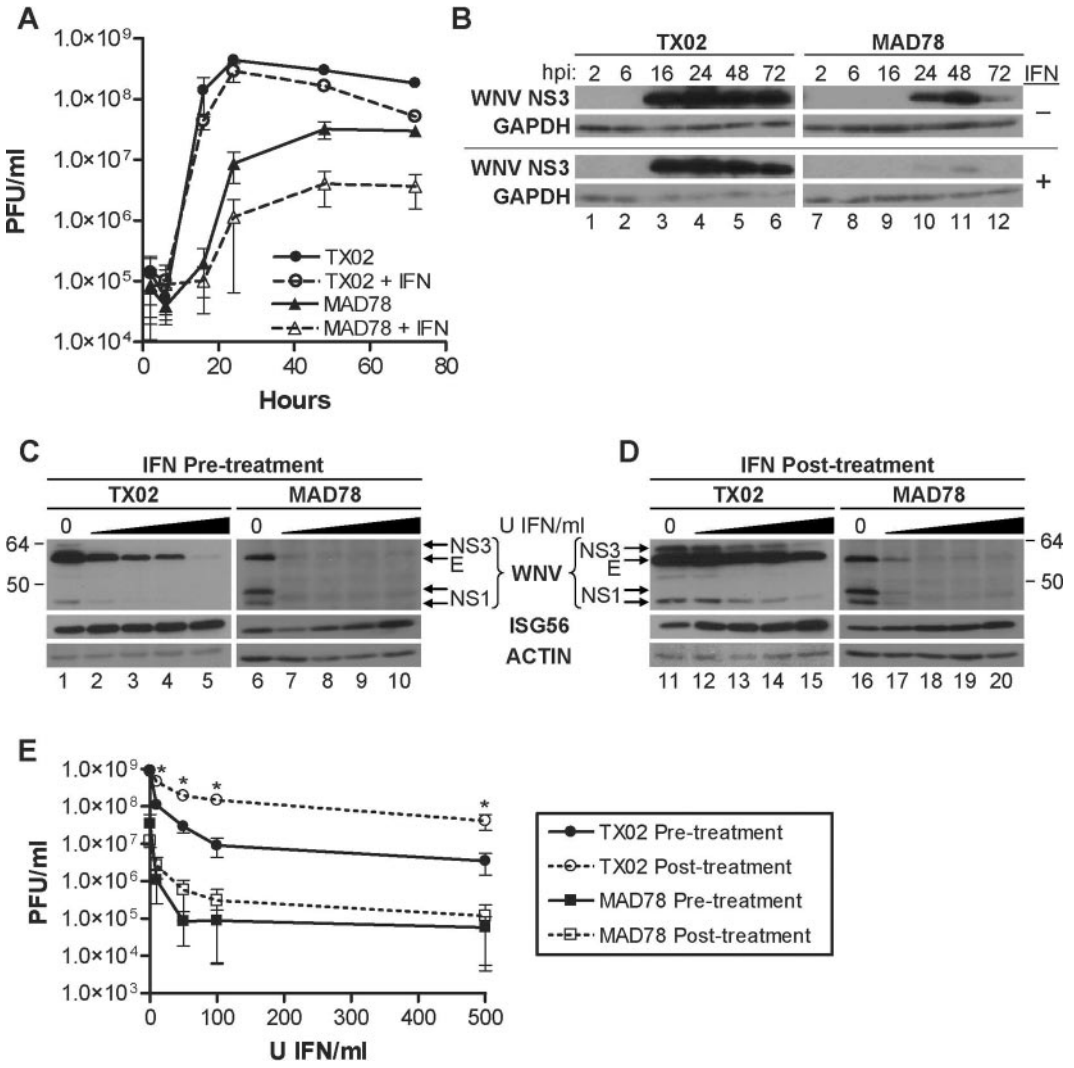

FIG. 3. IFN-α differentially controls growth of MAD78 and TX02. (A) A549 cells were infected (MOI = 1) with TX02 or MAD78 for 1 h. Following infection, medium containing 0 or 10 U IFN-α/ml was added to the cells. At 2, 6, 16, 24, 48, and 72 h postinfection, culture supernatants were collected and the titers of the viruses were determined by plaque assay on Vero cells. Results are expressed as the mean ± standard deviation. (B) Whole-cell lysates from samples shown in panel A were analyzed by immunoblotting for WNV and GAPDH protein abundance. hpi, hours postinfection. (C and D) A549 cells were treated with 0, 10, 50, 100, or 500 U IFN-α. (C) Cells were pretreated with IFN-α for 24 h prior to WNV infection. (D) Cells were first infected with WNV and then treated with IFN directly after virus adsorption. Cell cultures were maintained in the presence of the respective IFN-α dose for 24 h before being harvested. Whole-cell lysates were collected and analyzed by immunoblotting for the abundance of WNV proteins, ISG56, and actin. Cells were infected with TX02 or MAD78 at an MOI of 5. WNV proteins were detected with an antibody raised against the lineage I Egypt 1951 strain (GenBank accession number AF260968), revealing strain-specific differences in epitopes on the E and NS1 proteins. (E) For culture supernatants from the samples shown in panels C and D, the titers of the viruses were determined by plaque assay on Vero cells. Symbols: TX02, IFN-α pretreatment (●); TX02, IFN-α posttreatment (○); MAD78, IFN-α pretreatment (■); MAD78, IFN-α posttreatment (□). Results are expressed as the mean ± standard deviation. *, P value of <0.01 by unpaired t test.

for 24 h to induce an intracellular antiviral state. Cells were then infected in the presence of IFN-α-2a and maintained under these conditions for the duration of the experiment (IFN pretreatment) (Fig. 3C). Alternatively, cell cultures were infected with MAD78 or TX02, and increasing doses of IFN-α-2a were added to the growth medium following a 1-h virus adsorption (IFN posttreatment) (Fig. 3D). In the absence of exogenous IFN, WNV infection triggered the accumulation of ISG56, consistent with virus-induced activation of an IRF-3 dependent host response (15) (Fig. 3C and D, lanes 1, 6, 11, and 16). Treatment with as little as 10 U of IFN greatly reduced MAD78 protein abundance, whereas TX02 was refractory to this effect, with viral protein levels affected only slightly by treatment with 100 U IFN. Both IFN treatment regimens resulted in an approximate 1,000-fold decrease in infectious particle production in cells infected with MAD78, indicating that the timing of IFN treatment is not an important determinant of antiviral effectiveness against an IFN-sensitive strain of WNV (Fig. 3E). However, resistance of TX02 to IFN antiviral actions was significantly enhanced when IFN was added following virus infection ($P < 0.01$; unpaired t test), suggesting that products of TX02 are more effective than those of MAD78 at antagonizing IFN actions.

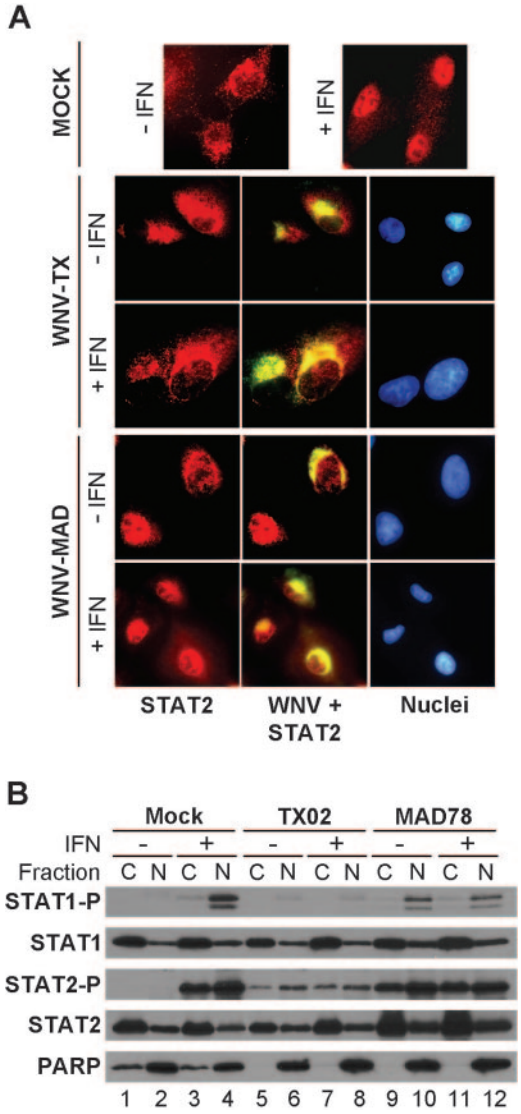

FIG. 4. TX02 prevents IFN-α-induced STAT1 and STAT2 nuclear translocation. (A) A549 cells were infected (MOI = 2) with TX02 or MAD78 or were left uninfected (MOCK). Twenty-four h postinfection, cells were treated with 1,000 U IFN-α for 1 h and then stained using primary antibodies directed against WNV or STAT2. Nuclei were stained with DAPI. Panels show representative confocal micrographs of images obtained (magnification, 40×). Top panels show STAT2 in mock-infected control cells. Images from infected cells show STAT2 (left column), STAT and WNV merged (middle column), and nuclei (right column). (B) A549 cells were infected (MOI = 5) with TX02 or MAD78. Twenty-four h postinfection, cells were left untreated or were treated with 1,000 U IFN-α for 1 h. Whole-cell lysates were fractionated into cytoplasmic and nuclear extracts and analyzed by immunoblotting using STAT- or phospho-STAT-specific antibodies. The fractionation of poly(ADP-ribose) polymerase (PARP) was monitored as a nuclear control protein. This shows that lanes 1 and 3 contained a residual level of nuclear material not present in lanes 5, 7, 9, and 11. P-, phosphorylated.

Differential regulation of JAK-STAT signaling by WNV. WNV has previously been shown to antagonize IFN signaling (17, 29), but the conservation of this regulation among strains with divergent virulence features has not been assessed. We therefore examined the effects of MAD78 and TX02 on IFN signaling processes. A549 cells were infected with MAD78 or TX02 for 24 h, treated with a high dose (1,000 U) of IFN-α-2a, and analyzed by confocal microscopy. In uninfected and MAD78-infected cells, STAT2 translocated to the nucleus following IFN treatment. However, the IFN-induced nuclear translocation of STAT2 was blocked in cells infected with TX02 (Fig. 4A). WNV infection triggers IFN production after infection (15), and in the absence of exogenous IFN treatment we found that STAT2 accumulated in the nuclei of cells infected with MAD78 but not TX02, suggesting that MAD78 is incapable of blocking even endogenous JAK-STAT signaling. Cellular fractionation further revealed the differential control of IFN signaling between WNV strains. Cultures of A549 cells infected with MAD78 or TX02 for 24 h were treated with high-dose IFN-α-2a for 1 h, after which cytoplasmic and nuclear extracts were prepared and subjected to immunoblot analysis to measure the abundance of the active, tyrosine-phosphorylated isoforms of STAT1 and STAT2 (Fig. 4B). In resting cells, STAT1 and STAT2 are expressed at low levels and shuttle between cytoplasmic and nuclear compartments (2, 33). Their levels increase through IFN-induced positive feedback signaling concomitantly with the nuclear accumulation of their active, phosphotyrosine isoforms (40). Consistent with this, IFN treatment stimulated the accumulation of phospho-STAT1 and phospho-STAT2 in extracts of mock-infected control cells, with high levels present in the nuclear fraction (Fig. 4B, lanes 1 to 4). MAD78 infection stimulated the expression and nuclear accumulation of phospho-STAT isoforms both in the absence and in the presence of IFN. In contrast, STAT protein accumulation was suppressed and occurred only at very low levels, regardless of IFN treatment in cells infected with TX02 (Fig. 4B, compare lanes 9 to 12 with lanes 5 to 8, respectively). Taken together, these results confirm that WNV has the capacity to induce a host response that includes STAT1 and STAT2 activation and that compared to what is seen for pathogenic WNV strains, the ability to suppress STAT activation is attenuated in MAD78.

To determine the level at which MAD78 was defective in blocking IFN-induced STAT phosphorylation, we examined the IFN-induced activation state of JAK-STAT components in cells infected with MAD78 or TX02 and treated with high-dose IFN-α-2a for 15 or 30 min. IFN treatment of uninfected cells induced the accumulation of the active, phosphotyrosine isoforms of Tyk2, STAT1, and STAT2 (Fig. 5A, lanes 1 to 3). TX02 prevented the IFN-induced tyrosine phosphorylation of Tyk2 and the downstream phosphorylation of STAT1 and STAT2. MAD78 infection resulted in very low-level accumulation of the active, phosphotyrosine isoform of Tyk2 and low-level accumulation of phospho-STAT2 in the absence or presence of exogenous IFN, whereas phospho-STAT1 was detected only after IFN treatment. In contrast to Tyk2 tyrosine phosphorylation, JAK1 tyrosine phosphorylation was detected in lysates of cells infected with TX02 or MAD78 even in the absence of exogenous IFN treatment (Fig. 5B). A basal level of phospho-JAK1 was found in all cells, while IFN treatment or WNV infection caused an accumulation of slower-migrating isoforms of phospho-JAK1, consistent with its activation (Fig. 5C). These results indicate that TX02 directs a blockade of Tyk2 but not Jak1 activation induced by IFN, and that this

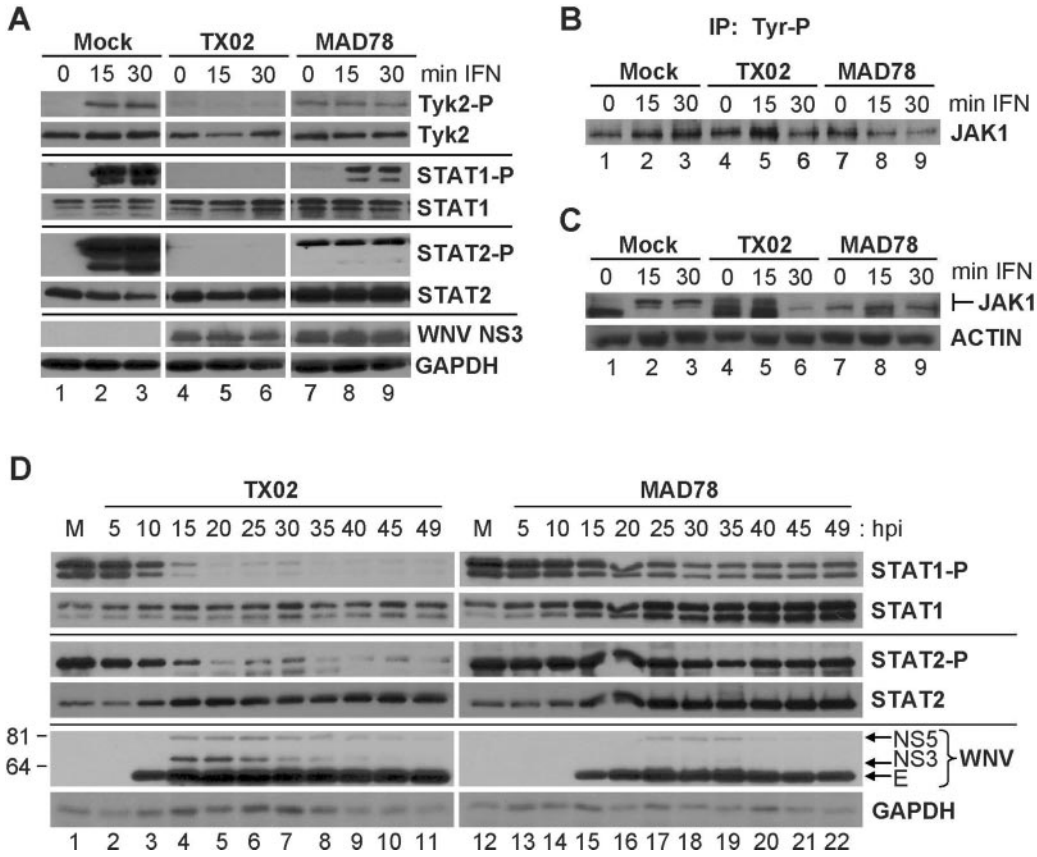

FIG. 5. MAD78 regulation of JAK-STAT signaling is attenuated. (A) A549 cells were mock infected (lanes 1 to 3) or infected (MOI = 5) with WNV (TX02, lanes 4 to 6; MAD78, lanes 7 to 9). Twenty-four h postinfection, cells were pulse treated with 1,000 U IFN-α for 0, 15, or 30 min, and whole-cell lysates were collected and analyzed by immunoblotting to determine WNV protein (NS3) abundance or the abundance of the active, tyrosine-phosphorylated (P) isoforms of Tyk2, STAT1, and STAT2. (B) A549 cells were mock infected or infected with TX02 or MAD78. Cells were then treated with 1,000 U IFN-α for the times indicated. Proteins were immunoprecipitated from whole-cell lysates by use of an antiphosphotyrosine antibody, and JAK1 immunoblot analysis was performed subsequently. (C) A549 cells were infected with TX02 or MAD78 and treated with IFN as described for panel A. Whole-cell lysates were analyzed for the presence of phospho-JAK1. (D) A549 cells were mock infected (M; lanes 1 and 12) or infected (MOI = 5) with TX02 (lanes 2 to 11) or MAD78 (lanes 13 to 22). In 5-h increments, cells were pulse treated with 1,000 U IFN-α for 30 min, and whole-cell lysates were collected and analyzed by immunoblotting to detect GAPDH, WNV, phosphotyrosine STAT isoforms, and total STAT1 or STAT2 abundance. Bars at left indicate the positions of molecular mass (kilodalton) standards. Arrows at right denote the positions of the indicated WNV proteins.

prevents the downstream phosphorylation and activation of STAT1 and STAT2. In contrast, MAD78 is attenuated in this function. To define the kinetics of this regulation, A549 cells were infected with TX02 or MAD78 and, at 5-h increments, were treated with IFN-α-2a for 30 min. Cell lysates were then collected and analyzed for the abundance of phosphorylated isoforms of STAT1 and STAT2. IFN treatment of mock-infected control cells induced high-level accumulation of the phosphotyrosine isoforms of STAT1 and STAT2 (Fig. 5D, lanes 1 and 12). In cells infected with MAD78, IFN responsiveness and the induction of STAT phosphorylation were preserved throughout the time course, though we did observe a partial suppression of phospho-STAT1 abundance that occurred in parallel with the accumulation of viral proteins. On the other hand, IFN treatment efficiently induced STAT phosphorylation during the first 5 h of infection with TX02, but this response was completely suppressed by 20 h, concomitant with the accumulation of viral proteins. This suggests that one or more viral proteins may influence IFN-induced JAK-STAT signaling during WNV infection and that these regulatory properties are defective in MAD78.

Control of IFN-α/β signaling is a determinant of WNV replication fitness in vitro and of virulence in vivo. Since MAD78 is attenuated in its ability to inhibit JAK-STAT signaling, we sought to determine the relative fitness levels of MAD78 and TX02 and whether or not WNV growth is enhanced in the absence of functional IFN-α/β signaling. Wild-type and congenic IFN-α/β receptor null ($IFNAR^{-/-}$) MEFs were infected with MAD78 or TX02, and viral growth was analyzed by a Vero cell plaque assay of the resulting culture supernatants. MAD78 yields were significantly enhanced ($P < 0.0001$; t test) 12-fold (Fig. 6A) in $IFNAR^{-/-}$ MEFs relative to infected wild-type MEFs. Interestingly, the yield of TX02 increased fivefold ($P < 0.01$; t test) in $IFNAR^{-/-}$ MEFs. This was not unexpected, since the block to JAK-STAT activation is most likely not absolute, as indicated by the very low-level accumulation of phosphorylated STAT2 in the nuclear fraction of TX02-infected cells treated with high-dose IFN (Fig. 4B, lane

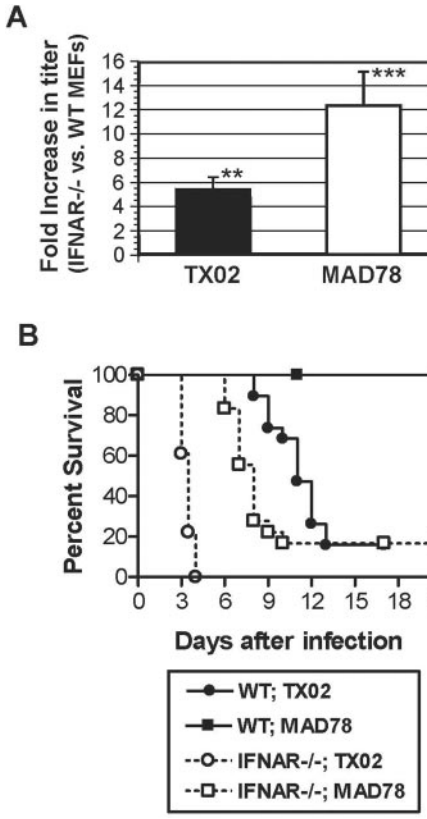

FIG. 6. JAK-STAT signaling controls WNV replication and virulence. (A) Wild-type (WT) and IFNAR$^{-/-}$ MEFs were infected with TX02 or MAD78, and the viral supernatant titers were determined by plaque assay on Vero cells. Columns represent the increases (n-fold) in titers of viral supernatant from wild-type MEFs to IFNAR$^{-/-}$ MEFs. **, $P < 0.01$; ***, $P < 0.0001$. (B) Groups of wild-type (WT) and congenic IFNAR$^{-/-}$ C57BL/6 mice were inoculated subcutaneously with 10^2 PFU of TX02 or MAD78 and monitored for survival. Results are plotted as percent survival for each group. Symbols: wild type, TX02 (●); wild type, MAD78 (■); IFNAR$^{-/-}$, TX02 (○); IFNAR$^{-/-}$, MAD78 (□).

8). Similar results were obtained from WNV infection of IFNAR-deficient U5A cells, STAT2-deficient U6A cells, and STAT1-deficient U3A cells (28, 31, 32; B. Keller and M. Gale Jr., unpublished observations). These results define JAK-STAT signaling and IFN actions as important determinants of viral fitness, and they indicate that viral regulation of these processes can enhance WNV replication in vitro.

To determine if the differential control of IFN signaling associated with the differential virulence of WNV, lethality studies of MAD78 or TX02 infection of wild-type and congenic IFNAR$^{-/-}$ C57BL/6 mice were performed (Fig. 6B). Subcutaneous infection of wild-type mice with 10^2 PFU of TX02 or MAD78 resulted in 86% lethality and 0% lethality, respectively ($n = 19$; $P < 0.0001$), confirming the attenuated nature of the MAD78 strain. Importantly, the virulence of MAD78 was unmasked in animals lacking IFNAR, where an 84% mortality rate ($n = 18$; median time to death, 8 days) was observed. In parallel studies of TX02 infection, we observed a 100% mortality of the IFNAR$^{-/-}$ mice ($n = 18$; $P < 0.0001$; median time to death, 3.5 days). Because its virulence in vivo is largely restored in mice that lack responsiveness to IFN-α/β, the relative absence of IFN antagonism by the MAD78 strain explains, in part, its attenuated phenotype. Nonetheless, because the virulence of MAD78 was not completely restored, additional as-yet-uncharacterized genetic variations must also contribute to the pathogenicity of WNV.

DISCUSSION

This study examined the relationship between IFN, virus replication, and viral pathogenesis of distinct WNV isolates that differ widely in terms of distribution pattern, pathogenesis, and epidemic behavior. Whereas MAD78 is a nonpathogenic lineage II strain with transmission behavior characteristic of endemic strains (5, 34), TX02 is a virulent strain of the current epidemic expansion of WNV lineage I in the Western Hemisphere. Our results provide evidence linking WNV virulence to control of the host cell JAK-STAT signaling pathway and overall resistance to the antiviral actions of IFN.

Sequence comparison of the complete open reading frames of MAD78 and TX02 to published complete WNV genomes confirmed the placement of MAD78 in lineage II (4, 5, 25, 26). Compared to epidemic lineage I WNV strains, MAD78 exhibited slow growth in vitro and an avirulent phenotype in vivo when inoculated peripherally into inbred C57BL/6 mice. TX02 clustered with emergent lineage I strains currently circulating in North America, and more specifically, with a subgroup of strains localized to the southwestern United States. In addition to sharing genotypic traits with other lineage I strains, TX02 also exhibited similar phenotypic growth and protein expression profiles in multiple human and mouse cell lines. Furthermore, when inoculated intraperitoneally into outbred Swiss-Webster mice, TX02 was nearly identical to NY 385-99 in terms of lethality. In agreement with others (3, 12), our data suggest very little genetic and phenotypic divergence has occurred among WNV strains circulating in North America. Thus, control of JAK-STAT signaling is likely a shared phenotype that confers virulence among emerging WNV strains while supporting virus replication and spread.

IFN-α/β plays an integral role in intracellular innate immunity as well as in the linkage of the innate immune response to cell-mediated defenses against virus infection. In order to replicate and spread, viruses direct processes to attenuate the initiation of IFN production and/or to antagonize the antiviral actions of IFN inside the host cell (23). The processes by which members of the family *Flaviviridae* regulate host defense and IFN actions vary widely. For example, hepatitis C virus and certain pestiviruses direct a blockade to IRF-3 activation, thus regulating the production of IFN by the infected cell (13, 20, 27, 30). WNV avoids activating IRF-3 early in infection but triggers its activation and IFN production during the late stages of infection, when viral proteins are abundant (14, 15). Consistent with this, infection of cells with TX02 or MAD78 conferred IRF-3 activation and its triggering of the host response (B. Fredericksen, B. Keller, and M. Gale, Jr., unpublished observations). In terms of TX02 infection, our results show that JAK-STAT activation by IFN becomes compromised in the host cell concomitantly with viral protein accumulation. In contrast, JAK-STAT signaling and IFN responsiveness remained largely intact in cells infected with MAD78,

suggesting that the ability of this virus to regulate IFN signaling actions is defective. This held true even late in infection, when MAD78 protein expression was at its maximum. The observations that (i) IFN treatment of cells prior to TX02 infection significantly reduced levels of virus production relative to IFN treatment after infection and (ii) the block in JAK-STAT signaling by TX02 occurred with the onset of viral protein expression both indicate that one or more WNV proteins can block IFN-induced signaling through the JAK-STAT pathway.

Results from several recent studies indicate that flaviviruses, including WNV, direct processes to regulate JAK-STAT signaling and IFN actions in the infected cell. Studies of WNV and Kunjin virus replicons provide evidence that viral protein(s) can direct a blockade of JAK-STAT signaling (17, 29, 39), and it is noteworthy that these replicons were derived from WNV strains that are virulent in vivo (4, 24). Others have identified various flavivirus nonstructural (NS) proteins as possible regulators of JAK-STAT signaling. The NS2A through NS4B proteins of Kunjin virus have been shown to regulate STAT phosphorylation (29), while the NS5 protein of Langat virus (a tick-borne flavivirus) and the NS2A, NS4A, and NS4B proteins from WNV and dengue virus can antagonize IFN action and regulate STAT1 phosphorylation when expressed alone or in *trans* during infection (8, 22, 35, 36). While these results may highlight distinct mechanisms by which different strains of flaviviruses control IFN actions, they collectively demonstrate that pathogenic strains of WNV can evade IFN through properties of JAK-STAT regulation. Tyk2 is essential for STAT1 and STAT2 phosphorylation in response to IFN-α/β receptor stimulation (40), and we found that infection of cells with TX02 resulted in a block of IFN-induced Tyk2 tyrosine phosphorylation and an abrogation of downstream STAT1 and STAT2 phosphorylation and nuclear translocation. Our data provide further support for a model in which one or more WNV NS proteins direct a blockade of IFN-induced Tyk2 activation and downstream STAT phosphorylation to attenuate the expression of ISGs that would otherwise control infection (17), thus allowing unimpeded virus replication and spread.

We have characterized MAD78, the first WNV strain shown to be incapable of regulating IFN-induced JAK-STAT signaling in infected cells, and shown that this associated with a lack of virulence upon virus challenge of wild-type animals. MAD78 also exhibited fitness that was lower overall than that of TX02. This attenuated MAD78 replication was augmented in vitro in cells lacking a functional IFN-α/β receptor, and a virulent phenotype was unmasked in vivo upon infection of IFNAR$^{-/-}$ mice. Taken together, these results imply that the normally avirulent phenotype of MAD78 (3, 23, 35) is due to overall reduced replication fitness and an inability of viral proteins to direct an effective JAK-STAT signaling blockade within the host cell. The reduced replication fitness of MAD78 may play a part in the IFN sensitivity of this strain early in infection, but no significant differences in infectious particle production were observed until late in infection (Fig. 3A). Furthermore, when MAD78 protein expression was at its maximum, JAK-STAT signaling remained largely intact (Fig. 5C), in contrast to what was seen for TX02. Lineage II WNV strains, including MAD78, differ from the emergent lineage I strains by approximately 22% at the nucleotide level but by only 7% at the amino acid level of encoded proteins (Keller and Gale, unpublished observations, and references 7 and 26), and these variations are scattered throughout the polyprotein. Of note is a Ser→Pro substitution at residue 156 of the MAD78 envelope protein (E protein) that abolishes the *N*-linked glycosylation motif (N-Y-T/S). Recently, Hanna et al. reported that WNV subviral particles lacking the E glycosylation site had a level of viral particle release 10-fold lower than that for strains with an intact N-Y-T/S motif (19). Expanding on this theme, a report by Borisevich et al. demonstrated that WNV strains containing a functional E glycosylation motif exhibited approximately 1.5-log increases in peak viral titers, irrespective of the origin of the NS genes (lineage I versus lineage II) (9). However, the effect of E glycosylation on virulence in vivo was minimal compared to the effect conferred by NS genes from different WNV strains. Results from these reports may explain the attenuated growth of MAD78 in vitro compared to that of strains that have an intact E glycosylation motif. Additionally, these studies further support our hypothesis that viral regulation of JAK-STAT signaling is a major determinant of WNV virulence in vivo. Since MAD78 appears to be attenuated both at the level of viral fitness and in terms of JAK-STAT regulation, it is likely that amino acid changes at multiple sites within the NS proteins account for its attenuated properties. Importantly, IFN imparts control of WNV virulence by limiting tissue tropism and the systemic dissemination of the virus while enhancing neuronal survival (38). Although these actions work through molecular mechanisms that are not yet known, they underscore the importance of the IFN response as the body's first line of defense against WNV infection and serve to define the processes and viral factors that determine WNV virulence and infection outcome.

Viral phenotypic traits that induce IFN and host defense processes could serve as a basis for attenuated vaccine approaches to confer protection against WNV infection in naïve populations. Hall et al. showed an attenuated strain of Kunjin virus was able to protect mice against lethal challenge with WNV (18). In this case, the attenuated viral phenotype was attributed to a single point mutation in the NS1 protein, and it is possible that attenuation could be mediated through loss of JAK-STAT signaling control. Such an approach could yield vaccine strains that replicate at levels controlled by IFN-α/β host defenses but that stimulate protective immunity against the virulence and neuroinvasiveness typical of current emergent WNV strains. The viral and host determinants that have allowed certain WNV strains to cause human epidemics in the recent past are largely unknown. It was reported that Toll-like receptor 3 signaling and subsequent production of tumor necrosis factor alpha are required for WNV entry into the brain (45). Additionally, several groups have reported on the role of E protein glycosylation in the neuroinvasiveness of WNV (6, 41). As mentioned earlier, MAD78 contains a Ser→Pro substitution in the E protein N-linked glycosylation motif. However, MAD78 retains a neuroinvasive phenotype but does so only in the absence of intact IFN-α/β signaling. While E glycosylation may play a role in particle assembly and infectivity (19), epitope masking, changing affinities for certain cellular receptors, or some other undefined mechanism, other viral and/or host determinants, including the ability to control the IFN system, likely contribute to the enhanced virulence of

epidemic WNV. The attenuated phenotype of MAD78 may provide a starting point for exploiting the link between viral stimulation of innate host defenses and immunity to infection.

ACKNOWLEDGMENTS

This work was supported by independent New Scholar Awards in Global Infectious Disease from the Ellison Medical Foundation to M.S.D. and M.G., a predoctoral fellowship from the Howard Hughes Medical Institute (M.A.S.), a National Institutes of Health Molecular Microbiology Training grant (B.C.K.), a Medical Scientist Training Program grant (B.C.K.), and NIH grant AI057568 (M.G.). M.G. is the Nancy C. and Jeffrey A. Marcus Scholar in Medical Research, in honor of Bill S. Vowell.

We thank Lisa Kinch for invaluable assistance with the phylogenetic analyses and Cindy Johnson for critical reading of the manuscript. All sequencing was performed in the DNA Sequencing Core Facility at The University of Texas Southwestern Medical Center.

We declare the absence of conflicting financial interests.

REFERENCES

1. **Adachi, J., and M. Hasegawa.** 1996. MOLPHY version 2.3: programs for molecular phylogenetics based on maximum likelihood. Comput. Sci. Monogr. **28:**1–150.
2. **Banninger, G., and N. C. Reich.** 2004. STAT2 nuclear trafficking. J. Biol. Chem. **279:**39199–39206.
3. **Beasley, D. W., C. T. Davis, H. Guzman, D. L. Vanlandingham, A. P. Travassos Da Rosa, R. E. Parsons, S. Higgs, R. B. Tesh, and A. D. Barrett.** 2003. Limited evolution of West Nile virus has occurred during its southwesterly spread in the United States. Virology **309:**190–195.
4. **Beasley, D. W., C. T. Davis, M. Whiteman, B. Granwehr, R. M. Kinney, and A. D. Barrett.** 2004. Molecular determinants of virulence of West Nile virus in North America. Arch. Virol. Suppl. **18:**35–41.
5. **Beasley, D. W., L. Li, M. T. Suderman, and A. D. Barrett.** 2002. Mouse neuroinvasive phenotype of West Nile virus strains varies depending upon virus genotype. Virology **296:**17–23.
6. **Beasley, D. W., M. C. Whiteman, S. Zhang, C. Y. Huang, B. S. Schneider, D. R. Smith, G. D. Gromowski, S. Higgs, R. M. Kinney, and A. D. Barrett.** 2005. Envelope protein glycosylation status influences mouse neuroinvasion phenotype of genetic lineage 1 West Nile virus strains. J. Virol. **79:**8339–8347.
7. **Berthet, F. X., H. G. Zeller, M. T. Drouet, J. Rauzier, J. P. Digoutte, and V. Deubel.** 1997. Extensive nucleotide changes and deletions within the envelope glycoprotein gene of Euro-African West Nile viruses. J. Gen. Virol. **78:**2293–2297.
8. **Best, S. M., K. L. Morris, J. G. Shannon, S. J. Robertson, D. N. Mitzel, G. S. Park, E. Boer, J. B. Wolfinbarger, and M. E. Bloom.** 2005. Inhibition of interferon-stimulated JAK-STAT signaling by a tick-borne flavivirus and identification of NS5 as an interferon antagonist. J. Virol. **79:**12828–12839.
9. **Borisevich, V., A. Seregin, R. Nistler, D. Mutabazi, and V. Yamshchikov.** 2006. Biological properties of chimeric West Nile viruses. Virology **349:**371–381.
10. **Burt, F. J., A. A. Grobbelaar, P. A. Leman, F. S. Anthony, G. V. Gibson, and R. Swanepoel.** 2002. Phylogenetic relationships of southern African West Nile virus isolates. Emerg. Infect. Dis. **8:**820–826.
11. **Cebulla, C. M., D. M. Miller, and D. D. Sedmak.** 1999. Viral inhibition of interferon signal transduction. Intervirology **42:**325–330.
12. **Ebel, G. D., J. Carricaburu, D. Young, K. A. Bernard, and L. D. Kramer.** 2004. Genetic and phenotypic variation of West Nile virus in New York, 2000–2003. Am. J. Trop. Med. Hyg. **71:**493–500.
13. **Foy, E., K. Li, C. Wang, R. Sumpter, Jr., M. Ikeda, S. M. Lemon, and M. Gale, Jr.** 2003. Regulation of interferon regulatory factor-3 by the hepatitis C virus serine protease. Science **300:**1145–1148.
14. **Fredericksen, B. L., and M. Gale, Jr.** 2006. West Nile virus evades activation of interferon regulatory factor 3 through RIG-I-dependent and -independent pathways without antagonizing host defense signaling. J. Virol. **80:**2913–2923.
15. **Fredericksen, B. L., M. Smith, M. G. Katze, P. Y. Shi, and M. Gale, Jr.** 2004. The host response to West Nile virus infection limits viral spread through the activation of the interferon regulatory factor 3 pathway. J. Virol. **78:**7737–7747.
16. **Goodbourn, S., L. Didcock, and R. E. Randall.** 2000. Interferons: cell signalling, immune modulation, antiviral response and virus countermeasures. J. Gen. Virol. **81:**2341–2364.
17. **Guo, J. T., J. Hayashi, and C. Seeger.** 2005. West Nile virus inhibits the signal transduction pathway of alpha interferon. J. Virol. **79:**1343–1350.
18. **Hall, R. A., D. J. Nisbet, K. B. Pham, A. T. Pyke, G. A. Smith, and A. A. Khromykh.** 2003. DNA vaccine coding for the full-length infectious Kunjin virus RNA protects mice against the New York strain of West Nile virus. Proc. Natl. Acad. Sci. USA **100:**10460–10464.
19. **Hanna, S. L., T. C. Pierson, M. D. Sanchez, A. A. Ahmed, M. M. Murtadha, and R. W. Doms.** 2005. N-linked glycosylation of West Nile virus envelope proteins influences particle assembly and infectivity. J. Virol. **79:**13262–13274.
20. **Horscroft, N., D. Bellows, I. Ansari, V. C. Lai, S. Dempsey, D. Liang, R. Donis, W. Zhong, and Z. Hong.** 2005. Establishment of a subgenomic replicon for bovine viral diarrhea virus in Huh-7 cells and modulation of interferon-regulated factor 3-mediated antiviral response. J. Virol. **79:**2788–2796.
21. **Jones, D. T., W. R. Taylor, and J. M. Thornton.** 1992. The rapid generation of mutation data matrices from protein sequences. Comput. Appl. Biosci. **8:**275–282.
22. **Jones, M., A. Davidson, L. Hibbert, P. Gruenwald, J. Schlaak, S. Ball, G. R. Foster, and M. Jacobs.** 2005. Dengue virus inhibits alpha interferon signaling by reducing STAT2 expression. J. Virol. **79:**5414–5420.
23. **Katze, M. G., Y. He, and M. Gale, Jr.** 2002. Viruses and interferon: a fight for supremacy. Nat. Rev. Immunol. **2:**675–687.
24. **Khromykh, A. A., and E. G. Westaway.** 1994. Completion of Kunjin virus RNA sequence and recovery of an infectious RNA transcribed from stably cloned full-length cDNA. J. Virol. **68:**4580–4588.
25. **Lanciotti, R. S., G. D. Ebel, V. Deubel, A. J. Kerst, S. Murri, R. Meyer, M. Bowen, N. McKinney, W. E. Morrill, M. B. Crabtree, L. D. Kramer, and J. T. Roehrig.** 2002. Complete genome sequences and phylogenetic analysis of West Nile virus strains isolated from the United States, Europe, and the Middle East. Virology **298:**96–105.
26. **Lanciotti, R. S., J. T. Roehrig, V. Deubel, J. Smith, M. Parker, K. Steele, B. Crise, K. E. Volpe, M. B. Crabtree, J. H. Scherret, R. A. Hall, J. S. MacKenzie, C. B. Cropp, B. Panigrahy, E. Ostlund, B. Schmitt, M. Malkinson, C. Banet, J. Weissman, N. Komar, H. M. Savage, W. Stone, T. McNamara, and D. J. Gubler.** 1999. Origin of the West Nile virus responsible for an outbreak of encephalitis in the northeastern United States. Science **286:**2333–2337.
27. **La Rocca, S. A., R. J. Herbert, H. Crooke, T. W. Drew, T. E. Wileman, and P. P. Powell.** 2005. Loss of interferon regulatory factor 3 in cells infected with classical swine fever virus involves the N-terminal protease, N^{pro}. J. Virol. **79:**7239–7247.
28. **Leung, S., S. A. Qureshi, I. M. Kerr, J. E. Darnell, Jr., and G. R. Stark.** 1995. Role of STAT2 in the alpha interferon signaling pathway. Mol. Cell. Biol. **15:**1312–1317.
29. **Liu, W. J., X. J. Wang, V. V. Mokhonov, P. Y. Shi, R. Randall, and A. A. Khromykh.** 2005. Inhibition of interferon signaling by the New York 99 strain and Kunjin subtype of West Nile virus involves blockage of STAT1 and STAT2 activation by nonstructural proteins. J. Virol. **79:**1934–1942.
30. **Loo, Y. M., D. M. Owen, K. Li, A. K. Erickson, C. L. Johnson, P. M. Fish, D. S. Carney, T. Wang, H. Ishida, M. Yoneyama, T. Fujita, T. Saito, W. M. Lee, C. H. Hagedorn, D. T. Lau, S. A. Weinman, S. M. Lemon, and M. Gale, Jr.** 2006. Viral and therapeutic control of IFN-beta promoter stimulator 1 during hepatitis C virus infection. Proc. Natl. Acad. Sci. USA **103:**6001–6006.
31. **Lutfalla, G., S. J. Holland, E. Cinato, D. Monneron, J. Reboul, N. C. Rogers, J. M. Smith, G. R. Stark, K. Gardiner, K. E. Mogensen, et al.** 1995. Mutant U5A cells are complemented by an interferon-alpha beta receptor subunit generated by alternative processing of a new member of a cytokine receptor gene cluster. EMBO J. **14:**5100–5108.
32. **McKendry, R., J. John, D. Flavell, M. Muller, I. M. Kerr, and G. R. Stark.** 1991. High-frequency mutagenesis of human cells and characterization of a mutant unresponsive to both alpha and gamma interferons. Proc. Natl. Acad. Sci. USA **88:**11455–11459.
33. **Meyer, T., and U. Vinkemeier.** 2004. Nucleocytoplasmic shuttling of STAT transcription factors. Eur. J. Biochem. **271:**4606–4612.
34. **Morvan, J., T. Besselaar, D. Fontenille, and P. Coulanges.** 1990. Antigenic variations in West Nile virus strains isolated in Madagascar since 1978. Res. Virol. **141:**667–676.
35. **Munoz-Jordan, J. L., M. Laurent-Rolle, J. Ashour, L. Martinez-Sobrido, M. Ashok, W. I. Lipkin, and A. Garcia-Sastre.** 2005. Inhibition of alpha/beta interferon signaling by the NS4B protein of flaviviruses. J. Virol. **79:**8004–8013.
36. **Munoz-Jordan, J. L., G. G. Sanchez-Burgos, M. Laurent-Rolle, and A. Garcia-Sastre.** 2003. Inhibition of interferon signaling by dengue virus. Proc. Natl. Acad. Sci. USA **100:**14333–14338.
37. **Reed, L. J., and H. Muench.** 1938. A simple method of estimating fifty per cent endpoints. Am. J. Hyg. **27:**493–497.
38. **Samuel, M. A., and M. S. Diamond.** 2005. Alpha/beta interferon protects against lethal West Nile virus infection by restricting cellular tropism and enhancing neuronal survival. J. Virol. **79:**13350–13361.
39. **Scholle, F., and P. W. Mason.** 2005. West Nile virus replication interferes with both poly(I:C)-induced interferon gene transcription and response to interferon treatment. Virology **342:**77–87.
40. **Sen, G. C.** 2001. Viruses and interferons. Annu. Rev. Microbiol. **55:**255–281.
41. **Shirato, K., H. Miyoshi, A. Goto, Y. Ako, T. Ueki, H. Kariwa, and I. Takashima.** 2004. Viral envelope protein glycosylation is a molecular determinant of the neuroinvasiveness of the New York strain of West Nile virus. J. Gen. Virol. **85:**3637–3645.

42. **Steele, K. E., M. J. Linn, R. J. Schoepp, N. Komar, T. W. Geisbert, R. M. Manduca, P. P. Calle, B. L. Raphael, T. L. Clippinger, T. Larsen, J. Smith, R. S. Lanciotti, N. A. Panella, and T. S. McNamara.** 2000. Pathology of fatal West Nile virus infections in native and exotic birds during the 1999 outbreak in New York City, New York. Vet. Pathol. **37:**208–224.
43. **Thompson, J. D., D. G. Higgins, and T. J. Gibson.** 1994. CLUSTAL W: improving the sensitivity of progressive multiple sequence alignment through sequence weighting, position-specific gap penalties and weight matrix choice. Nucleic Acids Res. **22:**4673–4680.
44. **Wang, F., Y. Ma, J. W. Barrett, X. Gao, J. Loh, E. Barton, H. W. Virgin, and G. McFadden.** 2004. Disruption of Erk-dependent type I interferon induction breaks the myxoma virus species barrier. Nat. Immunol. **5:**1266–1274.
45. **Wang, T., T. Town, L. Alexopoulou, J. F. Anderson, E. Fikrig, and R. A. Flavell.** 2004. Toll-like receptor 3 mediates West Nile virus entry into the brain causing lethal encephalitis. Nat. Med. **10:**1366–1373.
46. **Weber, F., G. Kochs, and O. Haller.** 2004. Inverse interference: how viruses fight the interferon system. Viral Immunol. **17:**498–515.